

# Prospects for Electroweak Precision Measurements and Triple Gauge Couplings at a Staged ILC

---

**Robert Karl\***

*Deutsches Elektronen-Synchrotron (DESY) and University of Hamburg*

*on behalf of the ILD concept group*

*E-mail: [robert.karl@desy.de](mailto:robert.karl@desy.de)*

In the absence of a direct discovery of new particles, precision measurements of the properties of known particles will provide the most powerful probe for phenomena beyond the Standard Model. Future electron positron linear colliders with polarised beams, like the International Linear Collider (ILC), will provide a unique laboratory for such measurements, complementary to hadron colliders.

In this contribution, we will review in particular the prospects for electroweak precision measurements, like the left-right asymmetry, as well as for measurements of charged triple gauge couplings based simulations of the ILD detector concept for the ILC. In all of these, the exact knowledge of the beam polarisation and the beam energy plays an important role. Therefore we will also discuss the precision determination of these accelerator parameters from collision data. We will pay special tribute to the most recent discussions concerning a possible first stage of the ILC operating at a center-of-mass energy of 250 or 350 GeV, but also comment of the full ILC running plan.

*EPS-HEP 2017, European Physical Society conference on High Energy Physics*

*5-12 July 2017*

*Venice, Italy*

---

\*Speaker.

## 1. Introduction

At lepton colliders, the initial state of the colliding particles is fully defined, including the orientation of their spins which is called polarization. This enables high precision studies of known particles like the Higgs boson or the top quark and a rich program of searches for the unknown, which is complementary to searches at the LHC.

The International Linear Collider (ILC) [1] is a planned electron-positron collider with center-of-mass energies of up to 500 GeV and a possible upgrade to 1 TeV. Its construction is under political consideration in the Kitakami region in the prefecture Iwate in Japan. At the ILC, both beams will be longitudinally polarized,  $|80\%|$  for  $e^-$ -beam and  $|30 - 60\%|$  for  $e^+$ -beam, including an individual switch of the polarization sign (helicity reversal) for both beams. This provides a choice between different spin configurations, which allows accurate measurements of the chiral structure of the electroweak interaction and possible new phenomena, e.g. Dark Matter.

The International Large Detector (ILD) is a concept for a detector at ILC. It is designed as a multi-purpose detector and optimized with a clear view on precision. This sets strong requirements on the ILD performance: A point resolution of the vertex detector better than  $3\ \mu\text{m}$ , a high tracking performance of  $\sigma_{1/p_T} \approx 2 \cdot 10^{-5} \text{ GeV}^{-1}$  and a jet-energy resolution of  $\sigma_E/E \approx 3 - 4\%$  which allows a separation of hadronic decays from  $Z$  and  $W$ . All studies were performed within the context of the ILD.

## 2. Beam Polarization Measurement

The usage of polarized beams provides great advantages for the ILC. It allows deep insights into the chiral structure of the weak-interaction for known and unknown particle as well as a sensitivity to additional observables (e.g. left-right-asymmetry). Furthermore, with polarized beams it is possible to suppress background processes and simultaneously increase signal processes, providing an enhancement of the signal to noise ratio.

However, since all event rates depend linearly on the polarization, it is important to provide a determination of the actual beam polarization at the permille-level in order to fully exploit the physics potential of the ILC [2]. This requirement can only be fulfilled by combining the fast time-resolved measurements of the laser-Compton polarimeters with an absolute scale calibration of the luminosity-weighted average polarization at the interaction point (IP) calculated from collision data.

Thus, the beam polarization will be measured online by 2 laser-Compton polarimeters [3] per beam. Thereby, for each beam, the upstream polarimeter is located 1.65 km before the IP, while the downstream polarimeter is located 150 m after the IP. In order to determine the polarization at the IP, the result of the polarimeter measurement is extrapolated to the IP via spin tracking [4]. For the absolute scale calibration, the luminosity-weighted averaged polarization is additionally calculated from collision data.

This study will focus on calculated from collision data using the minimization between the measured cross section  $\sigma_{\text{data}}$  and the theoretical expected cross section  $\sigma_{\text{theory}}$  [5]. Thereby, the cross sections are defined by:

$$\sigma_{\text{data}} := \frac{D - B}{\varepsilon \cdot \mathcal{L}_I} \quad (2.1)$$

$$\begin{aligned} \sigma_{\text{theory}} := & \frac{(1 - P_{e^-})(1 + P_{e^+})}{2} \cdot \sigma_{LR} + \frac{(1 + P_{e^-})(1 - P_{e^+})}{2} \cdot \sigma_{RL} \\ & + \frac{(1 - P_{e^-})(1 - P_{e^+})}{2} \cdot \sigma_{LL} + \frac{(1 + P_{e^-})(1 + P_{e^+})}{2} \cdot \sigma_{RR} \end{aligned} \quad (2.2)$$

41 With  $D$ ,  $B$ ,  $\varepsilon$ ,  $\mathcal{L}_I$  are the number of selected events, the expected number of background  
42 events, the detector selection efficiency and the integrated luminosity, respectively.  $P_{e^\pm}$  is the beam  
43 polarization of the  $e^\pm$ -beam and  $\sigma_{LR}$  corresponds to the chiral cross section with purely left-handed  
44 electrons and right-handed positrons. The four chiral cross sections are calculated by WHIZARD [6]  
45 considering ISR and the beam spectrum.

46 To maximize the precision on the luminosity-weighted averaged beam polarization, the standard  
47 model processes should have both a large left-right asymmetry  $A_{RL}^{LR}$  for a high sensitivity to the chi-  
48 ral structure and a high unpolarized cross section  $\sigma_0$  to increase the statistical precision. Thereby,  
49  $A_{RL}^{LR}$  and  $\sigma_0$  are defined by:

$$A_{RL}^{LR} := \frac{\sigma_{LR} - \sigma_{RL}}{\sigma_{LR} + \sigma_{RL}} \quad \sigma_0 := \frac{1}{4} \sum \sigma_{\{R,L\}} \quad (2.3)$$

50 The values for  $A_{RL}^{LR}$  and  $\sigma_0$  for a few suitable processes can be found in tab.1. For illustration,  
51 only the left-right asymmetry  $A_{RL}^{LR}$  was chosen in this study but in principle this approach would  
52 work similarly for all other left-right asymmetries ( eg.  $A_{LL}^{LR}$ , etc. ), as well. In leading order, the  
53  $W$ -pair production has the largest sensitivity to the beam polarization because it is only possible  
54 for left-handed electrons and right-handed positrons. Further more, it also has a sufficient large  
55 unpolarized cross section. As seen in tab.1, the s-channel  $Z$  exchange has a far lower sensitivity  
56 to the actual chiral structure but, due to the far larger unpolarized cross section, the sensitivity to  
57 the beam polarization is comparable to the  $W$ -pair production. The beam polarization can also  
58 be simultaneously determined from multiple processes including different channels in order to  
59 increase its precision.

Process [250 GeV]	$A_{RL}^{LR}$	$\sigma_0$ [pb]	
$e^+e^- \rightarrow W^+W^- \rightarrow q\bar{q}l\nu$	0.982	4.74	$l = \mu, \tau$ $q = u, d, c, s, b$
$e^+e^- \rightarrow Z \rightarrow q\bar{q}$	0.289	50.1	
$e^+e^- \rightarrow e^-\bar{\nu}W^+ \rightarrow e^-\bar{\nu}q\bar{q}$	0.983	1.29	
$e^+e^- \rightarrow e^+\nu W^- \rightarrow e^+\nu q\bar{q}$	0.983	1.29	
$\vdots$	$\vdots$	$\vdots$	

**Table 1:** A few processes with a large sensitivity to beam polarization and their corresponding values for the left-right asymmetry  $A_{RL}^{LR}$  and the unpolarized cross section  $\sigma_0$ , defined in eq. 2.3

### 60 3. Simultaneous Determination of the Chiral Cross Section

61 For the measurement of the luminosity-weighted averaged polarization from the total chiral  
62 cross sections, a precise knowledge of these cross sections is necessary. However, the beam po-

larization can also be determined from the chirality dependence of the differential cross section. Thus, by using differential cross section measurements, the beam polarization and the total chiral cross section can be determined simultaneously without relying on theoretical calculations alone. For the measurement of the total chiral cross sections the following parametrization was used: For each process and channel, a parameter  $\alpha$  scales the unpolarized cross section and another parameter  $\beta$  allows for a shift in the asymmetry. They are defined as:

$$A \longrightarrow A + \beta \qquad \sigma_0 \longrightarrow \alpha \cdot \sigma_0 \qquad (3.1)$$

14 standard model processes including their channels were used in this study. This results in a 32 parameter fit: four parameters for the beam polarization and two pseudo- nuisance parameters per process and channel, as defined in eq.3.1. Thereby, all 28 pseudo- nuisance parameters are correctly determined without loss of precision on the beam polarization. The results for the statistical precision of all parameters can be found in tab.2. As it is shown, the statistical precision of a permille-level on all parameters is well achievable. Note that the permille-level goal on the beam polarization precision is exceeded because these results only include the statistical precision.

$\chi^2 / \text{NDF}: 753.43 / 708$							
$\Delta P_{e^-}^-$	3.4	$\Delta P_{e^-}^+$	1.3	$\Delta P_{e^+}^-$	3.9	$\Delta P_{e^+}^+$	2.9
$\Delta\alpha_{W^+}(e\nu l\nu)$	12	$\Delta\alpha_{W^-}(e\nu l\nu)$	12	$\Delta\beta_{W^-}(e\nu l\nu)$	13	$\Delta\beta_{W^+}(e\nu l\nu)$	6.2
$\Delta\alpha_{W^+}(e\nu q\bar{q})$	7.5	$\Delta\alpha_{W^-}(e\nu q\bar{q})$	7.5	$\Delta\beta_{W^-}(e\nu q\bar{q})$	7.6	$\Delta\beta_{W^+}(e\nu q\bar{q})$	3.6
$\Delta\alpha_{WW}(q\bar{q}q\bar{q})$	5.6	$\Delta\alpha_{WW}(l\nu l\nu)$	12	$\Delta\beta_{WW}(l\nu l\nu)$	4.9	$\Delta\beta_{WW}(q\bar{q}q\bar{q})$	1.6
$\Delta\alpha_{WW}(l\nu q\bar{q})$	5.4	$\Delta\alpha_{ZZ}(q\bar{q}q\bar{q})$	10	$\Delta\beta_{ZZ}(q\bar{q}q\bar{q})$	12	$\Delta\beta_{WW}(l\nu q\bar{q})$	1.4
$\Delta\alpha_{ZZ}(llll)$	28	$\Delta\alpha_{ZZ}(llq\bar{q})$	9.8	$\Delta\beta_{ZZ}(llq\bar{q})$	12	$\Delta\beta_{ZZ}(llll)$	34
$\Delta\alpha_{ZZWW}(q\bar{q}q\bar{q})$	5.8	$\Delta\alpha_{ZZWW}(l\nu l\nu)$	12	$\Delta\beta_{ZZWW}(l\nu l\nu)$	8.1	$\Delta\beta_{ZZWW}(q\bar{q}q\bar{q})$	2.9
$\Delta\alpha_Z(q\bar{q})$	1.6	$\Delta\alpha_Z(l^+l^-)$	2.4	$\Delta\beta_Z(l^+l^-)$	4.2	$\Delta\beta_Z(q\bar{q})$	3.3

**Table 2:** Results for the absolute uncertainty on the polarization and the pseudo nuisance parameters  $\alpha$ ,  $\beta$ , defined in eq.3.1, in  $10^{-4}$  from the simultaneous fit at  $\sqrt{s} = 250 \text{ GeV}$  and  $\mathcal{L}_I = 2000 \text{ fb}^{-1}$

#### 4. Measurement of Triple Gauge Couplings (TGC) at an $e^+e^-$ Collider

Lepton colliders are well suited to measure electroweak triple gauge couplings. However, the measurement of these couplings also has a large sensitivity to the actual beam polarization. Thus, the polarization measurement would significantly affect the TGC determination and vice versa. Therefore, it is necessary to measure anomalous TGC and the beam polarization simultaneously. This can be achieved in a similar way as the simultaneous calculation of the total chiral cross section, described in sec. 3.

For a center-of-mass energy of 500 GeV, the simultaneous measurement of the beam polarization and anomalous TGC was studied using  $W$ -pair production in the semileptonic channel [7]. This study was performed with a full detector simulation of the ILD detector concept and the precision on the three anomalous TGCs  $g_1^Z$ ,  $\kappa_\gamma$  and  $\lambda_\gamma$  were determined simultaneously within a Effective

87 Field Theory (EFT) approximation including second order terms. This study was repeated at a  
 88 center-of-mass energy of 1 TeV, also with the full ILD detector simulation [8].  
 89 These analysis provide two reference points for TGC precision at different center-of-mass energies.  
 90 The goal is an approximation on the TGC precision at 250 GeV by extrapolating the 500 GeV re-  
 91 sults to 250 GeV. Therefore, three scaling factors were considered; the first is the statistical scaling  
 92  $f_{\text{stat}}$  which is just given by  $1/\sqrt{N}$  and the second is the actual sensitivity to the TGCs which is as-  
 93 sumed to scale with  $M_W^2/s$ . The third scaling factor  $f_{\text{det}}$  is related to the energy dependence of the  
 94 detector acceptance. Such a factor is hard to predict, and thus it is determined by the comparison  
 95 between the 500 GeV and 1 TeV results. The final scaling factors are shown in eq. 4.1.

$$\Delta c_i(\sqrt{s}) = \Delta c_i(500 \text{ GeV}) \cdot f_{\text{stat}}(\sqrt{s}; \mathcal{L}_I) \cdot f_{\text{theo}}(\sqrt{s}) \cdot f_{\text{det},i}(\sqrt{s}) \quad (4.1a)$$

$$f_{\text{stat}}(\sqrt{s}; \mathcal{L}_I) = \sqrt{\frac{500 \text{ fb}^{-1} \cdot \sigma(500 \text{ GeV})}{\mathcal{L}_I \cdot \sigma(\sqrt{s})}}; \quad f_{\text{theo}}(\sqrt{s}) = \frac{(500 \text{ GeV})^2}{s} \quad (4.1b)$$

$$f_{\text{det},\Delta g}(\sqrt{s}) = 0.85 + \frac{0.15}{500 \text{ GeV}} \cdot \sqrt{s}; \quad f_{\text{det},\Delta \lambda}(\sqrt{s}) = 0.63 + \frac{0.37}{500 \text{ GeV}} \cdot \sqrt{s} \quad (4.1c)$$

$$f_{\text{det},\Delta \kappa}(\sqrt{s}) = 1; \quad (4.1d)$$

96 The achievable precision of the TGC measurement is shown in tab.3. At the ILC, a sub-permille-  
 97 level on anomalous TGC precision can already be reached in the first stage of ILC with 250 GeV.  
 98 This is roughly 2 orders of magnitude better than the current best limit on anomalous TGCs, as  
 99 shown in fig.1.

ILD full simulation [7]		Extrapolations		
$E_{\text{CMS}}$	500 GeV	250 GeV	350 GeV	H-20 [9]
$\Delta g_1^Z$	$4.3 \cdot 10^{-4}$	$8.1 \cdot 10^{-4}$	$5.0 \cdot 10^{-4}$	$5.0 \cdot 10^{-4}$
$\Delta \kappa_\gamma$	$4.4 \cdot 10^{-4}$	$9.6 \cdot 10^{-4}$	$5.5 \cdot 10^{-4}$	$5.7 \cdot 10^{-4}$
$\Delta \lambda_\gamma$	$4.1 \cdot 10^{-4}$	$7.8 \cdot 10^{-4}$	$5.0 \cdot 10^{-4}$	$5.1 \cdot 10^{-4}$

**Table 3:** Achievable precision of the Triple Gauge Couplings measurement for  $\mathcal{L}_{\text{ILC}} = 2 \text{ ab}^{-1}$  at the ILC

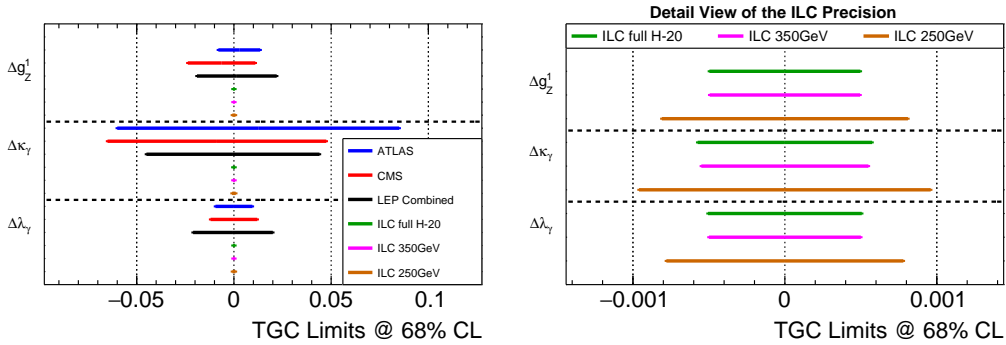


**Figure 1:** Comparison of the reachable TGC precision of the ILC, shown in tab.3, with the final results from LEP combined from ALEPH, L3 and OPAL results [10] and the LHC TGC limits for  $\sqrt{s} = 8 \text{ TeV}$  data and an integrated luminosity of  $\mathcal{L}_I = 20.3 \text{ fb}^{-1}$  and  $\mathcal{L}_I = 19.4 \text{ fb}^{-1}$  for ATLAS and CMS, respectively [11]

100 **References**

- 101 [1] **ILC Project**, T. Behnke et al., eds., *International Linear Collider Reference Design Report Volume 1:*  
102 *Executive Summary*. 2013
- 103 [2] Annika Vauth, Jenny List. *Beam Polarization at the ILC: Physics Case and Realization*,  
104 Spin Physics (SPIN2014), International Journal of Modern Physics: Conference Series, 29 February  
105 2016,  
106 <http://www.worldscientific.com/doi/pdf/10.1142/S201019451660003X>
- 107 [3] Jenny List, Annika Vauth, and Benedikt Vormwald:  
108 *A Quartz Cherenkov Detector for Compton-Polarimetry at Future  $e^+e^-$  Colliders*  
109 (<https://bib-pubdb1.desy.de/record/221054>)  
110 *A Calibration System for Compton Polarimetry at  $e^+e^-$  Colliders*  
111 (<https://bib-pubdb1.desy.de/record/289025>)
- 112 [4] Moritz Beckmann, Jenny List, Annika Vauth, and Benedikt Vormwald:  
113 *Spin transport and polarimetry in the beam delivery system of the international linear collider*  
114 (<http://iopscience.iop.org/article/10.1088/1748-0221/9/07/P07003/pdf>)
- 115 [5] Robert Karl, Jenny List, *Polarimetry at the ILC*, arXiv:1703.00214
- 116 [6] The WHIZARD Event Generator, *A program system designed for the efficient calculation of*  
117 *multi-particle scattering cross sections and simulated event samples*, <https://whizard.hepforge.org/>
- 118 [7] I. Marchesini, *Triple Gauge Couplings and Polarization at the ILC and Leakage in a Highly Granular*  
119 *Calorimeter*, PhD Thesis, University of Hamburg, 2011 (DESY-THESIS-2011-044),  
120 <http://www-library.desy.de/cgi-bin/showprep.pl?desy-thesis-11-044>
- 121 [8] Aura Rosca, *Measurement of the charged triple gauge boson couplings at the ILC*,  
122 Nuclear and Particle Physics Proceedings 273-275 (2016) 2226-2231,  
123 <http://dx.doi.org/10.1016/j.nuclphysbps.2015.09.362>
- 124 [9] Jenny List, *Running Scenarios for the ILC*,  
125 LC Forum / Terascale Annual Meeting November 17-18, 2015, DESY  
126 ([http://pubdb.xfel.eu/record/289187/files/jlist\\_lcforum\\_1511.pdf?version=1](http://pubdb.xfel.eu/record/289187/files/jlist_lcforum_1511.pdf?version=1))
- 127 [10] T. L. C. ALEPH, DELPHI, L3, OPAL, and the LEP TGC Working Group, *A combination of results*  
128 *on charged triple gauge boson couplings measured by the LEP experiments*,  
129 LEPEWWG/TGC/2005-01.
- 130 [11] LHC limits on anomalous triple and quartic gauge couplings in comparison of the running  
131 experiments: <https://twiki.cern.ch/twiki/bin/view/CMSPublic/PhysicsResultsSMPaTGC>